Desalination and Water Treatment
www.deswater.com

doi: 10.5004/dwt.2022.28082

247 (2022) 108–120
January

Adsorption characterization and mechanism of aluminum based chitosan/zeolite molecular sieve composite for fluoride removal

Yunan Gao[a,*], Shui Liu[b]

[a]*School of Environmental and Chemical Engineering, Foshan University, Foshan 528225, China, email: gaoyunan01@163.com*
[b]*Foshan Water and Environmental Protection Co., Ltd., Foshan Water, Foshan 528000, China, email: hitwater@163.com*

Received 27 July 2021; Accepted 18 December 2021

ABSTRACT

Groundwater containing high concentration of fluoride has made great concern in China. Many researchers are eager to look for an applicable method for fluoride removal. Adsorption process is broadly recognized as a low-cost, high-efficient and environmental-friendly technology. In this research, a novel adsorbent prepared by aluminum sulfate modified chitosan/zeolite molecular sieve (AC-Z) composites was used to remove fluoride from synthetic solutions. The fluoride adsorption performance of AC-Z adsorbents was investigated by factors of dose (0.5–7 mg/100 mL), contact time (0.5–12.0 h), temperature (10°C–35°C), solution pH (3–11), initial fluoride concentration (5.0–50.0 mg/L) and co-existing anions (Cl^-, CO_3^{2-}, SO_4^{2-}) in series of batch experiments. Scanning electron microscopy (SEM), energy dispersive spectroscopy (EDS), Brunauer–Emmett–Teller and Fourier transform infrared spectroscopy (FTIR) were used to analyze the structure and morphology of the AC-Z adsorbents. The AC-Z adsorbents with fluoride removal efficiency of 93.1% were processed under conditions of initial concentration 10 mg/L, dose 2 g/100 mL, contact time 8 h, pH value 7 and temperature 20°C. The kinetic studies indicated that fluoride adsorption followed the pseudo-second-order kinetics well (R^2 = 0.999), and adsorption isotherms can be well described by Freundlich model (R^2 = 0.988). Thermodynamic studies showed the fluoride adsorption was spontaneous and endothermic. The results of this preliminary study indicated that AC-Z was a potential and efficient treatment option for groundwater with fluoride pollution.

Keywords: Aluminium sulfate; Chitosan; Zeolite molecular sieve; Fluoride

1. Introduction

Groundwater is the major and preferred source of drinking water in some rural and urban areas in China. However, groundwater is getting polluted due to the ever-growing population, industrialization, urbanization and unskilled utilization of water resources [1]. Many studies have reported that the groundwater in North and Northeast areas of China (Fig. 1) had a fluoride concentration above the guideline value [2]. An evidence from speciation analysis and geochemical modeling showed that groundwater fluoride concentrations ranged from 0.18 to 10.21 mg/L, and approximately 65% of groundwater fluoride was higher than the standards in North China Plain [3]. According to the World Health Organization (WHO), the maximum acceptable concentration of fluoride ions in drinking water is less than 1.5 mg/L [4]. The limit fluoride concentration of China Drinking Water Standard is less than 1.0 mg/L [5]. In some developed cities of China, the requirements for fluorine concentration are more stringent, like Shenzhen Drinking Water Standards, the limit fluorine concentration is less than 0.8 mg/L [2].

A clean water source with an appropriate fluorine concentration is an important prerequisite for ensuring healthy

* Corresponding author.

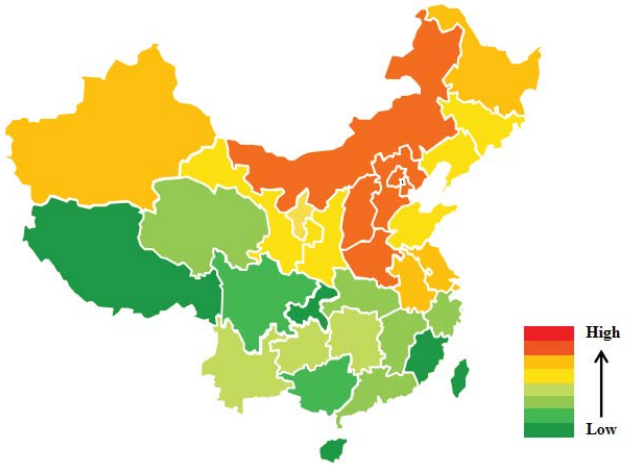

Fig. 1. Fluoride pollution area of groundwater in China.

drinking water for human daily life [6]. The appropriate amount of fluorine is beneficial for the body to synthesize CaF_2 for normal mineralization of bones and formation of dental enamel [7]. In some country, like Australia, fluoride is added to the clean water at the final step of drinking water treatment process, because the lack of fluorine in the human body can easily lead to tooth decay [8]. In addition, it will also affect some physiological functions of the human body. However, its excessive intake may result in slow, progressive crippling scourge known as fluorosis [9]. If the concentration of fluoride is more than 2 mg/L in groundwater, the necessary advanced technology needs to be used in drinking water treatment process.

Many researches perform on defluorination to remove the excess of fluoride effectively from drinking water [10], including coagulation-precipitation [11], membrane process [12], ion-exchange [13], electrodialysis [14] and adsorption [15]. However, most of these techniques with some drawbacks didn't work cost-effectively for actual application. The drawbacks of these methods are the generation of high disposal waste, presence of co-ions in water [11], expensive for application, the problem of fouling, scaling and membrane degradation [16]. Comparatively, adsorption process is broadly used for fluoride removal because it is simple to use, low cost, less maintenance, high removal efficiency [17]. Alumina is considered as the most effective adsorbent for fluoride removal from water. Table 1 summarized the comparative analysis of the fluoride removal by alumina and aluminum-based adsorbents of recent years. Although several attempts have shown promising adsorption capacities for fluoride, however, the main disadvantage of aluminum-based materials were the high residual aluminum remained in water after defuoridation [18–20]. For this reason, current studies are focused on combining aluminum with other environmentally friendly materials to improve the removal of fluoride while reduce the release of aluminum in water.

Chitosan is a naturally-derived polysaccharide. Due to its characteristics of wide source, safe and nontoxic, environment-friendly, it has wide application prospect in the field of water treatment, such as heavy metals, phenolic compound and dyes [21]. Chitosan is frequently modified in order to improve its physicochemical properties and can be cross-linked with the other media to form multi-functional composite materials [22]. Burillo et al. [23] synthesized chitosan hydrogels (net-CS) to remove fluoride from groundwater, the removal capacity of net-CS was 0.150 mg/g for F after 50 h. Jagtap et al. [24] investigated chitosan based mesoporous alumina and found that the removal efficiency and adsorption capacity was 78% and 8.26 mg/g for 5 mg/L concentration of fluoride, respectively. However, these chitosan-based powder material was not easy to recycle, which limited its application. Zeolite molecular sieve is a kind of synthetic sodium zeolite, with a Si-Al-Si framework tetrahedral structure, and large specific surface area. Because of its nanopore size, zeolites molecular sieves are more effective at treating anionic species than other water treatment materials. Aluminum coated natural zeolite (Alc-STI) has been investigated for water defluoridation previously. Aluminol, silanol functional groups, and the hydroxyl on Alc-STI had co-operative actions for F^- ion exchange which enhanced the adsorption capacity [25]. It was feasible to study aluminum-based chitosan or aluminum-based zeolite materials for fluoride removal, however limited works have been published the performance of aluminum, chitosan and zeolite combining together for fluoride removal.

In this research work, aluminium coated onto the chitosan/zeolite molecular sieve particles (AC-Z) were synthesized for fluoride removal. To check the performance of AC-Z adsorbent to remove fluoride from aqueous solution, batch experiments have been done to obtain the removal efficiency and adsorption capacity at different dose,

Table 1
Alumina adsorbents for fluoride adsorption

Adsorbent	pH	*F* Concentration	Contact time	Dose	Temp.	Removal efficiency	Adsorption capacity	References
AA	4.4	15 mg/L	90 min	4.5 g/L	25°C	94%	8.4 mg/g	[18]
MCA	7	10 mg/L	3 h	8 g/L	25°C	98%	0.16 mg/g	[19]
MAA	7	12 mg/L	1 h	10 g/L	20°C	95%	0.76 mg/g	[20]
net-CS	7.6–8.3	0.23–2.33 mg/L	50 h	8 g/L	25°C	40%–46%	0.15 mg/g	[23]
CMA	3–9	5 mg/L	24 h	4 g/L	30°C	78%	8.26 mg/g	[24]
Alc-STI	6.5	10 mg/L	6 h	6 g/L	22°C	–	1.6 mg/g	[25]

Notes: AA = Acidic alumina; MCA = Magnesium dioxide coated alumina; MAA = Modified immobilized activated alumina; net-CS = net-chitosan hydrogels; CMA = Chitosan based mesoporous alumina 450; Alc-STI = Aluminum-coated stilbite.

contact time, pH value, temperature, initial concentration and co-exiting anions. The study focused on properties of AC-Z adsorbent before and after fluoride adsorption by scanning electron microscopy (SEM), energy dispersive spectroscopy (EDS), Brunauer–Emmett–Teller (BET) and Fourier transform infrared spectroscopy (FTIR) analysis. Adsorption kinetics, isotherms and thermodynamics were also invited to study the mechanism of AC-Z defluoridation.

2. Experimental procedure

2.1. Chemicals materials

The AC-Z adsorbent was prepared by aluminum sulfate ($Al_2(SO_4)_3 \cdot 18H_2O$, >99.0%, Sinopharm Chemical Reagent Co., Ltd., China), chitosan (>90% deacetylated, Shenyang Sinopharm Group, China) and zeolite molecular sieve (NaA type, BET surface area 13.395 m^2/g, pore volume 0.041 cm^3/g, average pore diameter 25.897 nm, Shanghai New Molecular Sieve Co., Ltd., China). The fluoride polluted water samples were prepared by sodium fluoride (NaF, >98.0%, Sinopharm Chemical Reagent Co., Ltd., China). Fluoride analysis was used SPADNS agent purchased from HACH, USA. pH was adjusted by hydrochloric acid (HCl, 1 mol/L) and sodium hydroxide (NaOH, 1 mol/L) were supplied by Sinopharm Chemical Reagent Co., Ltd., China. All chemicals were of analytical reagent grade.

2.2. Preparation of AC-Z

AC-Z adsorbent was synthesized according to the procedures of Fig. 2. The first step: zeolite molecular sieve (5 g) was added into a 250 mL flask containing 7 g/L chitosan solution, then 2 mL of acetic acid (2 vol.%) was dropped into the zeolite molecular sieve and chitosan solution with continuous oscillation. The composites were stirred at the speed of 140 rpm for 12 h at temperature of 20°C, then dried in the oven at 70°C for 3 h. The second-step: the dried composites obtained in the first step were added into 100 mL aluminum sulfate solution (0.2 mol/L), and were oscillated at the speed of 140 rpm for 12 h at 20°C. Then, washed in distilled water, dried in the oven at 70°C for 3 h and stored in a desiccator until use.

2.3. Characterization

The characterizations of AC-Z adsorbents before and after fluoride ion adsorption were analyzed by SEM, EDS, BET and FTIR. The specific surface area analysis (BET) was performed by using a Quantachrome Autosorb-iQ (USA) instrument. The morphology (SEM) and elemental mapping imaging (EDS) of AC-Z adsorbents was characterized by S4800 HITACHI (Japan) instrument. FTIR spectra from the range 4000–400 cm^{-1} were obtained on FT-IR spectrophotometer (Tensor 27, Burker, German).

2.4. Adsorption experiment

Adsorption experiments were performed by batch tests to study the different factors on fluoride ion removal of AC-Z adsorbents, including the dosage (0.5, 1.0, 1.5, 2.0, 3.0, 4.0, 5.0, 6.0, 7.0 g/100 mL), contact time (0.5, 1.0, 2.0, 4.0, 6.0, 8.0, 10.0, 12.0 h), pH value (3, 4, 5, 6, 7, 8, 9, 10, 11), temperature (283, 288, 293, 298, 303, 308 K), initial concentration (5.0, 10.0, 20.0, 50.0 mg/L) and co-exiting anions (Cl^-, CO_3^{2-}, SO_4^{2-}) in solutions. Fluoride concentration of water samples (except initial concentration test) were average 10 mg/L, which were simulated from fluoride contaminated groundwater in Liaoning province, China. The application experiments of AC-Z adsorbents were used the fluoride-contaminated groundwater acquired from the Kangping city. The collected samples were examined in the laboratory for CO_3^-, SO_4^{2-}, Cl^- utilizing standard approaches suggested via Standard for groundwater quality (GB/T 14848). The concentration of Fe^{2+}, Mn^{2+} and the residual aluminum in solution was determined using an inductively coupled plasma mass spectrometer (Agilent ICP-MS 7500, USA). Fluoride concentration was determined by UV-spectrophotometer (D3900, HACH, USA). pH value of water samples in adsorption experiments was adjusted by 0.1 M HCl or 0.1 M NaOH. Fluoride ion concentrations of treated water were measured after reaching adsorption equilibrium with rotating speed of 140 rpm. All adsorption batch tests were performed three times.

The adsorption capacity (q_e, mg/g) and fluoride removal efficiency (R, %) were calculated as described in Eqs. (1) and (2).

$$q_e = \frac{(C_0 - C_e)V}{m} \tag{1}$$

$$R = \frac{(C_0 - C_e)}{C_0} \times 100\% \tag{2}$$

where C_0 (mg/L) is the initial F^- concentration of the adsorbent. C_e (mg/L) is the equilibrium F^- concentration. m (g) is the mass of the AC-Z adsorbent. V (L) is the volume of the water sample. The analysis results were the average values of three replicates.

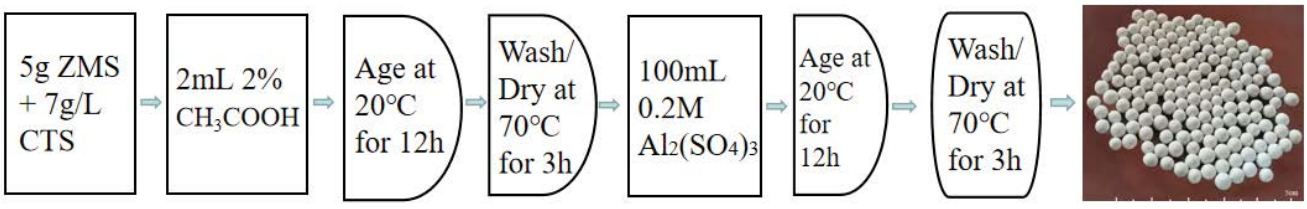

Fig. 2. AC-Z adsorbent synthesis procedures; ZMS: zeolite molecular sieve; CTS: chitosan.

Adsorption isotherm experiments were studied by varying initial fluoride concentration of 2, 4, 6, 8, 10, 12 mg/L in contact with 100 mL of a 2.0 g AC-Z adsorbents respectively during 12 h at 140 rpm, 7.0 pH value and 20°C temperature. Adsorption kinetic experiments were conducted by batch experiment at pH 7.0 with initial fluoride concentration (10.0 mg/L). Several water samples were added with 2.0 g/100 mL AC-Z adsorbents stirred at the speed of 140 rpm, respectively. Water samples were shaken for different time intervals (15, 30, 60, 120, 180, 240, 300, 360, 420, 480, 540, 600, 660 and 720 min), then each fluoride concentration was analyzed. Adsorption thermodynamic experiments were conducted in the same way as kinetics except with different temperature at 283, 288, 293, 298, 303, 308 K with stirred time 12 h, respectively.

Regeneration experiments were conducted with several different chemicals to optimize the best regenerant. 2.0 g of AC-Z particles saturated with fluoride were placed in 100 mL of 1 mol/L HCl, 1 mol/L NaOH, 1 mol/L $AlCl_3$, 1 mol/L Na_2SO_4, 1 mol/L NaCl solution, respectively. Each sample was shaken at 140 rpm and room temperature for 8 h. Then, adsorbed particles after regeneration by different chemicals were rinsed with deionized water and dried at a temperature of 70°C for 3 h. Adsorption capacities and fluoride removal rates of each sample were analyzed to determine the best regenerant. Then, the life of the AC-Z adsorbent was determined by the running times of recovered adsorbent washed by regenerant. After each run of the AC-Z adsorbent saturated with fluoride, they were washed with best regenerant as the way of regeneration experiments. The recovered adsorbent could then be reused in the next run. The running times and fluoride removal efficiency of each run were analyzed to determine the adsorption ability of AC-Z adsorbent.

3. Results and discussion

3.1. Effect of AC-Z dose

The effect of AC-Z adsorbent dose on fluoride adsorption at the initial concentration of 10 mg/L, pH value of 7 and temperature of 20°C is shown in Fig. 3a. It was shown that the fluoride removal efficiency of AC-Z was increased from 44.1% to 93.1% with the increase in the dose from 0.5 g/100 mL to 2.0 g/100 mL, respectively. Also, after a dose of 2.0 g/100 mL, the fluoride removal efficiency was maintained at 94.5%–95.9%. Compared to removal efficiency, the adsorption capacity decreased with the dose increasing. There was a sharp decline in the amount of adsorption capacity after a dose of 2.0 g/100 mL. Due to the concentration of fluoride in the solution was limited, with increasing the dose of AC-Z adsorbent, accumulation

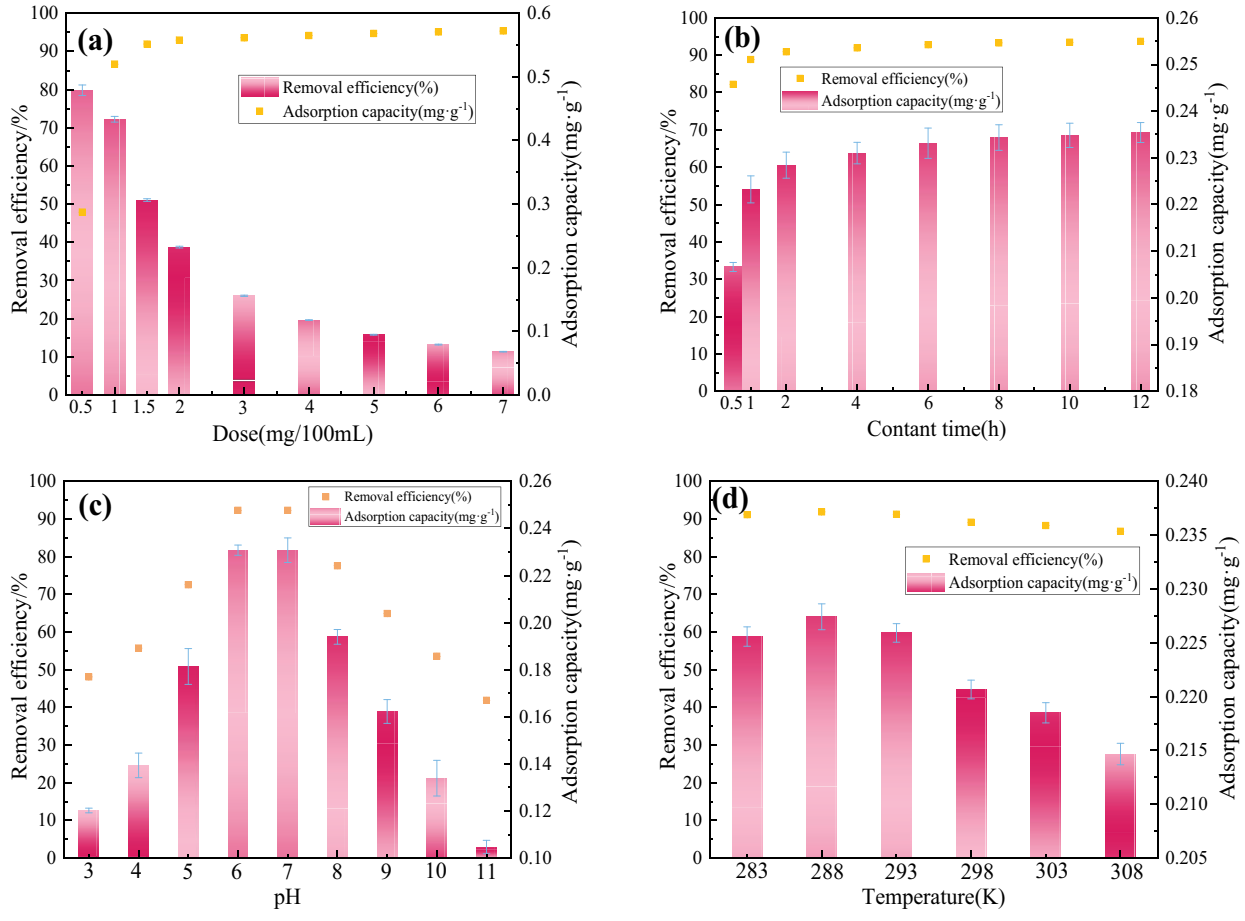

Fig. 3. Effect of (a) AC-Z dose, (b) contact time, (c) pH, and (d) temperature on fluoride adsorption.

of adsorbent could reduce the removal efficiency [26]. Therefore, the optimal dose was chosen to be 2.0 g/100 mL. The treated water sample was 0.7 mg/L at this dose, which was less than 1.0 mg/L of the water quality standard.

3.2. Effect of contact time

The effect of contact time was illustrated at the dose of 2.0 g/100 mL, initial concentration of 10 mg/L, pH value of 7 and temperature of 20°C (Fig. 3b). It was clearly seen that the removal efficiency increased from 74.3% to 94.4% with increasing the contact time from 0.5 to 12 h. The adsorption capacities were increased strongly in the first 4h with the amount increasing from 0.37 to 0.47 mg/g. The fluoride ions in water were adsorbed rapidly on the surface of the adsorbent during the initial contact time which accelerated the removal efficiency. This can be attributed to the fact that at the beginning of the process, there are many active sites for adsorption [27]. As the reaction was carried out for 8 h, the adsorption capacity and removal efficiency were almost unchanged, indicating that the adsorption reaction had reached equilibrium.

3.3. Effect of pH

Initial pH value of water sample was one of the most important factors during fluoride adsorption process, because it controlled the surface charge, surface binding sites of the adsorbents [28]. The adsorption capacity and removal efficiency of AC-Z adsorbent in 10 mg/L fluoride ions at different pH conditions are shown in Fig. 3c. It can be obviously seen that the removal efficiency of AC-Z for fluoride were found to be high with 93.5% and 92.5% at pH 6 and 7 respectively. Adsorption capacity were also at high levels, which indicated the AC-Z adsorbent was suitable for neutral water condition and applicable in practice. However, in the acidic and alkaline water environment, the removal efficiency and adsorption capacity of AC-Z adsorbent were not high. When pH value was below 6, hydrogen ion (H^+) in water combined with fluoride ion (F^-) to form HF, the presence of a large amount of hydrogen ion inhibited the hydrolysis of HF, making the AC-Z adsorbent unable to react with fluoride ions [29]. When pH value was above 7, the electrostatic repulsion of fluoride ions to the negatively charged surface of the AC-Z, making the hydroxyl ions (OH^-) and the fluoride ion (F^-) competitive in alkaline solution [30]. The hydroxyl ions competed with fluoride ions for the active sites on the particles which reduced the adsorption ability of the AC-Z adsorbent [31,32]. This adsorbent was not quite suitable for acidic or basic condition.

3.4. Effect of temperature

Effect of temperature on adsorption capacity and fluoride removal efficiency of AC-Z adsorbent is shown in Fig. 3d. The adsorption process was repeated at the above best condition (2.0 g/100 mL of dose, 8 h of contact time, 7 of pH value) at different temperature respectively. It was found with increasing the temperature from 283 K to 293 K, the removal efficiency of fluoride and adsorption capacity were both at a high level with the amount around 91%–92% and 0.460–0.462 mg/g. On the other hand, the temperature increasing to 308 K caused a sharp decrease of fluoride removal (less than 85%) on AC-Z adsorbent, this may due to the decease of surface ion exchange and electrostatic interactions when the temperature was above 308 K [33]. Taking the actual groundwater temperature and economic cost into consideration, the optimal adsorption temperature was determined to be 288–293 K (15°C–20°C).

3.5. Effect of initial concentration

The effect of initial fluoride concentration of adsorption (5, 10, 20, 50 mg/L) was carried out and the results of removal efficiency and adsorption capacity are shown in Fig. 4a and b. It can be seen that the removal efficiency had a sharp increase in the first 1 h, especially for the

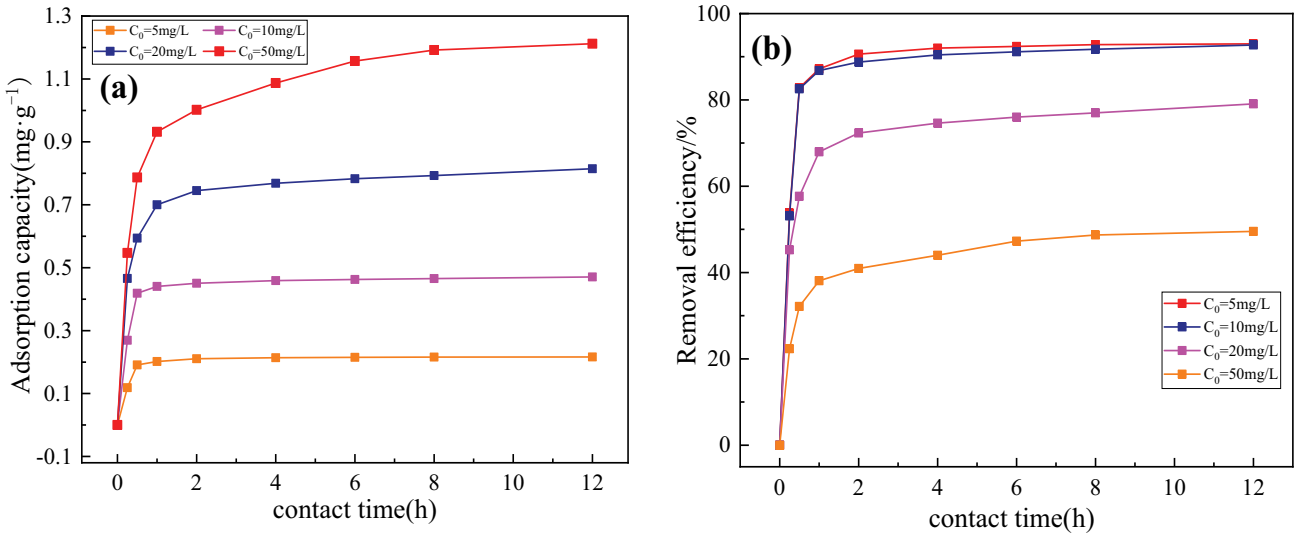

Fig. 4. Effect of initial concentration on fluoride adsorption capacity (a) and removal efficiency (b).

initial concentration of 5 and 10 mg/L. During this time, most of the fluoride was adsorbed on the AC-Z adsorbents with the removal efficiency of 85% for both 5 and 10 mg/L. With increasing the contact time, a marginal increase was observed up to over 2 h. The adsorption efficiency was faster in the initial 1 h of reaction, because of sufficient active sites made it easier for the fluoride ions to adhere to the surface of the particles [34]. With the increasing time, the concentration of fluoride in solution was decreased, this might be due to saturation of active sites or decrease in the fluoride concentration in the solution [35]. The adsorption ability of AC-Z increased with increasing concentration of fluoride ions in water. As the initial concentration increased from 5 to 50 mg/L, the equilibrium adsorption capacity was 0.22, 0.47, 0.82 and 1.21 mg/g, respectively.

3.6. Effect of co-existing anions

In actual polluted water, there are some co-ions like Cl^-, CO_3^{2-}, SO_4^{2-} presented with F^-. These co-ions interfere in adsorption of F^- for active adsorption sites. Fig. 5 illustrates the effect of these three co-existing anions on fluoride removal by adding different concentration of these anions in the fluoride (10 mg/L) polluted solution. As the Cl^- concentration in solution increased from 0 to 500 mg/L, the removal efficiency of fluoride decreased from 93.62% to 88.56%, and the adsorption capacity decreased from 0.47 to 0.44 mg/g, respectively. This indicates that the adsorption of fluoride was not adversely affected by the presence of Cl^- ion. In contrast, CO_3^{2-} and SO_4^{2-} affected the adsorption of fluoride ion more than Cl^-. The increase of carbonate concentration in water would increase the pH value of the water, as the results of pH effect shown (3.3), the AC-Z adsorbent had poor fluoride adsorption ability for basic condition. Also, the ratio of charge to the radius (z/r) of the anions had a close correlation with their affinity, and SO_4^{2-} (2/0.230) had higher z/r values, so it had a greater affinity to compete with fluoride ions, which z/r value is 1/0.140 [36,37]. The order of removal efficiency of the three ions on the fluoride adsorption effect was $SO_4^{2-} > CO_3^{2-} > Cl^-$.

3.7. Adsorption kinetics

In order to understand the mechanism of fluoride adsorption on AC-Z adsorbent, pseudo-first-order kinetic (Fig. 6a) and pseudo-second-order kinetic (Fig. 6b) were studied to examine the adsorption data. The experiments were conducted at AC-Z dose of 2 g/100 mL, contact time of 8 h, initial concentration of 10 mg/L, pH value of 7 and temperature of 20°C. Both kinetic models were liner fitted, and R^2 for pseudo-first-order kinetic and pseudo-second-order kinetic models as shown in Table 2 were 0.9615 and 0.9999 respectively, revealing that the goodness fit of pseudo-second-order kinetic model for the adsorption. Also, it was found that the value of q_e obtained by pseudo-second-order kinetic model was 0.481 mg/g, which was

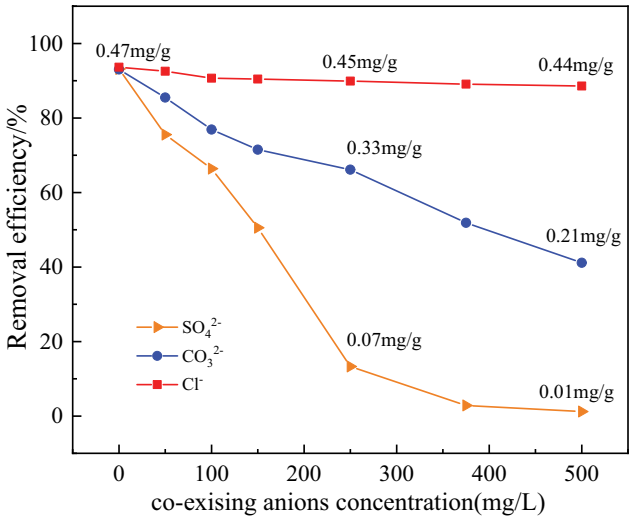

Fig. 5. Effect of co-existing anions on fluoride adsorption.

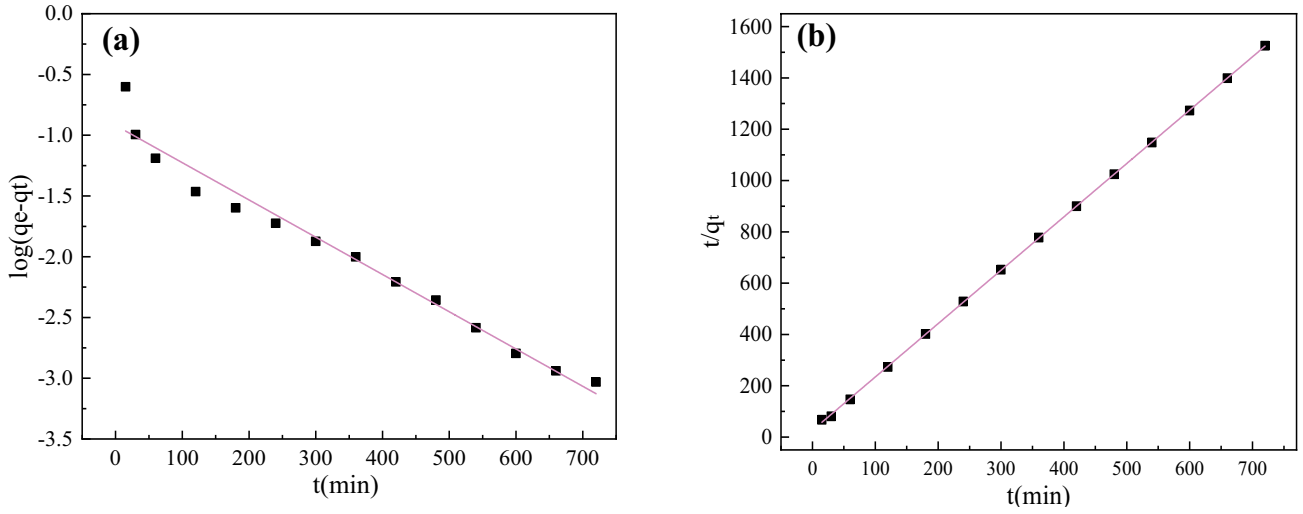

Fig. 6. Pseudo-first-order kinetic (a) and pseudo-second-order kinetic (b).

Table 2
AC-Z adsorption kinetic parameters

Pseudo-first-order model			Pseudo-second-order model		
$\log(q_e - q_t) = \log q_e - \frac{k_1}{2.303}t$			$\frac{t}{q_t} = \frac{1}{k_2 q_e^2} + \frac{t}{q_e}$		
q_e	k_1	R^2	q_e	k_2	R^2
0.120	0.007	0.9615	0.481	0.164	0.9999

Note: t is the contact time (min); q_e and q_t are fluoride adsorption amounts at time of equilibrium and at any contact time t (min) respectively, (mg/g); k_1 (min^{-1}) and k_2 (mg g^{-1} min) are the constants of the quasi-first-order kinetic model and pseudo-second-order kinetic model respectively; R^2 is correlation coefficient.

consistent with the adsorption capacity results obtained in previous effects experiments (Fig. 3b). Therefore, pseudo-second-order kinetic could be utilized to explore the adsorption kinetics of the AC-Z adsorbent.

3.8. Adsorption isotherms

The fluoride adsorption process was explained by Langmuir (Fig. 7a) and Freundlich (Fig. 7b). The parameters for the two isotherms are shown in Table 3. The experiments were conducted at dose of 2.0 g/100 mL, contact time of 8 h, pH of 7 and temperature of 20°C. Langmuir isotherm model is often applied for monolayer adsorption onto a surface containing a certain number of identical sites [38]. Freundlich isotherm model is applied for multilayer adsorption onto a heterogeneous surface [35]. As shown in Fig. 7 and Table 3, both isotherms fit well in the adsorption data. R^2 for the two isotherms were 0.9803 and 0.9886 respectively, which illustrated Freundlich was fit better. The Freundlich constant indicated adsorbent multilayer heterogeneous surface [38]. Table 3 shows the constant n between 1 and 10 and the positive value of K_L confirmed the favorable adsorption.

3.9. Adsorption thermodynamic

The fluoride adsorption on AC-Z adsorbent was studied at 283, 288, 293, 298, 303, and 308 K with F^- concentration of 10 mg/L, contact time of 8h and pH of 7. As the results of previous temperature effect study shown (Fig. 3d), with increasing the temperature from 15°C to 35°C, there was a slight decrease in fluoride adsorption. And according to the data in Table 4, $\Delta H°$ was calculated from the van't Hoff plot of ln$K$ vs. 1/T. The negative value of enthalpy ($\Delta H°$) showed that the adsorption process was exothermic [39]). From the negative Gibb's free energy values ($\Delta G°$), it can be seen that the adsorption process was obvious spontaneity and feasibility [40]. The negative value of $\Delta S°$ showed the decrease in the randomness of the entire system during the fluoride adsorption of AC-Z adsorbent [41].

3.10. SEM, EDS and BET

Fig. 8a–d show the surface morphology of AC-Z adsorbent. Fig. 8a and b show the images of AC-Z adsorbent before fluoride adsorption at 5000 and 10000 magnification, respectively. The original surface was formed with more concavo-convex structure [42]. Cube-like sphere shapes

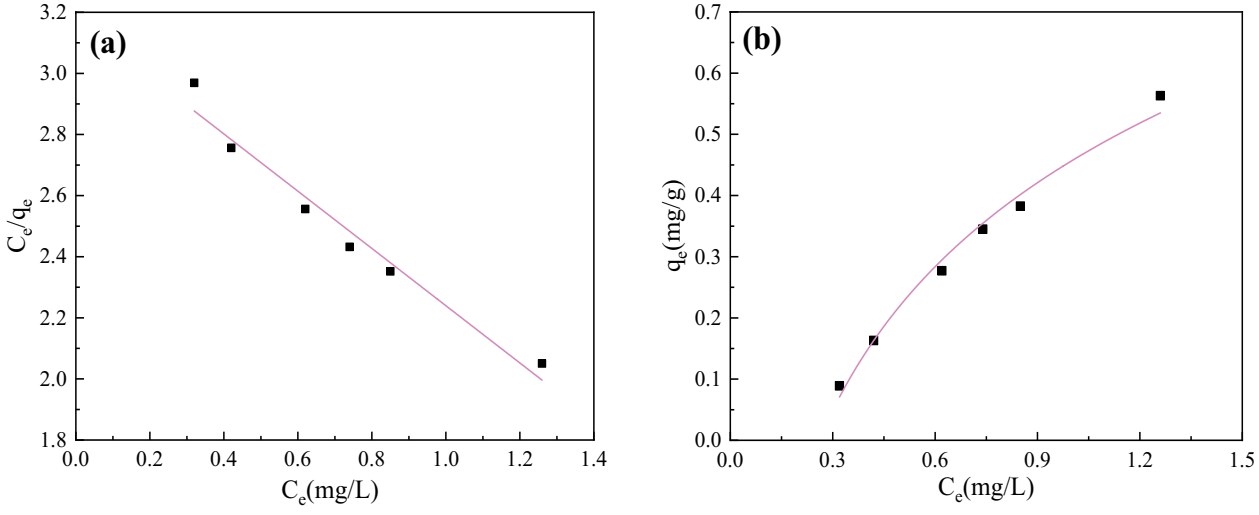

Fig. 7. The adsorption of fluoride by Langmuir (a) and Freundlich (b) isotherm models.

Table 3
Langmuir and Freundlich adsorption isotherm parameters

Langmuir adsorption isotherm model			Freundlich adsorption isotherm model		
$\frac{C_e}{q_e}=\frac{C_e}{q_m}+\frac{1}{q_m K_L}$			$q_e = K_F C_e^{1/n}$		
q_m	K_L	R^2	K_F	n	R^2
1.282	0.310	0.9803	2.848	2.16	0.9886

Note: q_e (mg/g) is the equilibrium adsorption capacity, q_m (mg/g) is the maximum fluoride adsorption capacity, C_e (mg/L) is the equilibrium concentration of fluoride, K_L (L/mg) is the constant of Langmuir adsorption isotherm model, K_F ((mg/g)/(mg/L)$^{1/n}$) is the constant of Freundlich adsorption isotherm model, n is the adsorption intensity, R^2 is correlation coefficient.

Table 4
Thermodynamic parameters

	$K=\frac{(C_0-C_e)}{C_e\times m}=\frac{q_e}{C_e}$		
	$\Delta G^\circ = -RT\ln K = \Delta H^\circ - T\Delta S^\circ$	$\ln K = \frac{\Delta S^\circ}{R} - \frac{\Delta H^\circ}{RT}$	
T (K)	ΔG° (kJ/mol)	ΔH° (kJ/mol)	ΔS° (kJ/mol K)
283	–0.4373		
288	–0.4232		
293	–0.4045		
298	–0.3785	–1.751	-4.617×10^{-3}
303	–0.3572		
308	–0.3192		

Note: ΔG° (kJ/mol) is the standard Gibbs free energy, ΔH° (kJ/mol) is the standard enthalpy change, ΔS° (kJ/mol K) is the standard entropy change, K is the apparent equilibrium constant, R is a universal gas constant 8.314 J/(mol K), T (K) is absolute temperature, C_0 (mg/L) and C_e (mg/L) are the initial concentration and equilibrium concentration of fluoride, respectively. q_e (mg/g) is adsorption capacity.

were presented on the AC-Z surface. These spherical surfaces were rough and had an average size of 5.8 × 6.4 μm. After adsorption of fluoride, except the surface structure of AC-Z (Fig. 8c and d) became rougher, there was no other change. Fig. 9 and Table 5 show EDS analysis of AC-Z adsorbent before and after fluoride adsorption. It was observed that C (8.76 wt.%), N (9.89 wt.%), O (47.80 wt.%), Na (4.34 wt.%), Al (13.37%) and Si (14.67%) were the main compensation elements in AC-Z adsorbent. New element of F (1.41 wt.%) was presented after adsorption which can be attributed to adsorption process. The decrease in the weight percentage of aluminum from 13.37% to 11.17% indicated that aluminum may had a reaction with fluoride in solution.

BET analysis of zeolite molecular sieve and AC-Z are shown in Table 6. The BET surface area, pore volume, and average pore diameter of AC-Z were 47.0075 m^2/g, 0.1198 cm^3/g and 11.1767 nm, respectively. The surface area of AC-Z was greater than zeolite molecular sieve, most likely due to the fact that the chitosan and aluminum sulfate, which were scattered on the zeolite molecular sieve bed, enlarging its surface [24].

3.11. FTIR analysis

The FTIR spectra of zeolite molecular sieve (a), chitosan (b), AC-Z before (c) and after fluoride adsorption (d) are recorded in Fig. 10. In the spectrum of zeolite molecular sieve (line a), the band at 3,467 cm^{-1} and 552 cm^{-1} were caused by the stretching vibration of the X–OH and O–X–O groups (X means Si/Al), respectively, which were the basic tetrahedral skeleton of zeolite molecular sieve [26]. In the spectrum of chitosan (line b), the bands at 1,473 and 1,653 cm^{-1} were attributed to the stretching vibrations of the $–CH_3$ group and N–H group, respectively [43]. These two bands indicated the active groups of the chitosan. The FTIR spectra of the AC-Z before fluoride adsorption (line c), showed typical bands of X–OH, N–H, $–CH_3$ and O–X–O groups at 3,446; 1,663; 1,473 and 552 cm^{-1}, respectively, which indicated the functional groups of chitosan and zeolite molecular sieves were loaded onto the surface of the AC-Z [44]. An increase in the intensity of peak at 3,446 cm^{-1} was observed that more active sites of Al–OH groups were loaded on the surface of the AC-Z after aluminium

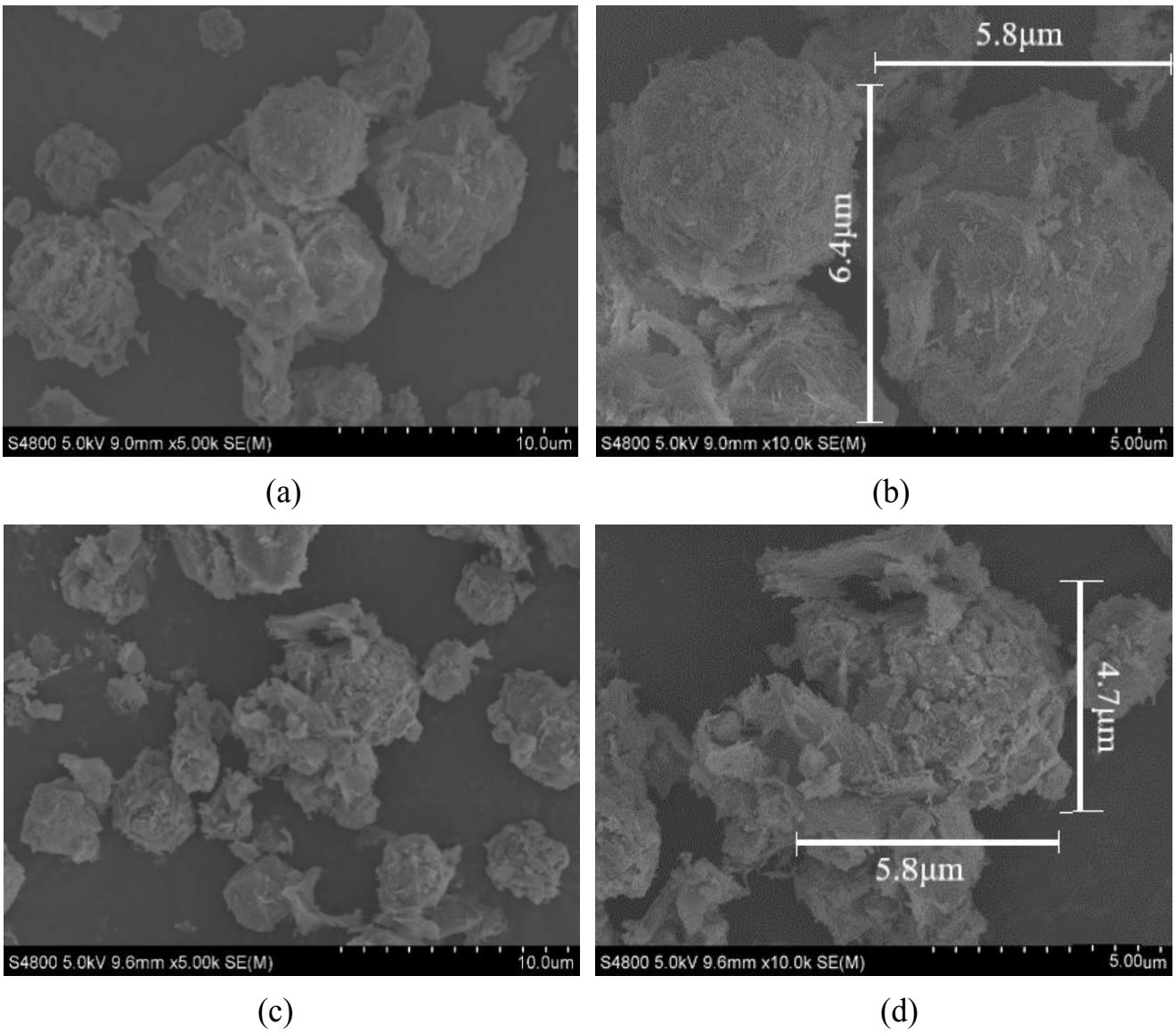

Fig. 8. Image changes before and after AC-Z adsorption of fluorine (a) AC-Z (×5000), (b) AC-Z (×10000), (c) AC-Z after fluoride adsorption (×5000), and (d) AC-Z after fluoride adsorption (×10000).

Table 5
Element percentage of AC-Z before and after fluoride adsorption

Samples	Element (wt.%)	C	N	O	Na	Al	Si	K	Ca	F	Total amount
AC-Z	Weight percentage	8.76	9.89	47.80	4.34	13.37	14.67	–	0.50	–	100.00
	Atomic percentage	12.46	12.06	51.02	3.23	6.36	8.91	–	0.21	–	
Fluoride adsorbed AC-Z	Weight percentage	8.27	9.57	46.85	4.63	11.17	15.21	0.28	0.61	1.41	100.00
	Atomic percentage	11.88	11.67	54.71	3.89	8.01	10.47	0.14	0.30	2.02	

sulfate modification [44]. After adsorption of fluoride (line d), the change in intensities of function group of –OH from 3,446 cm^{-1} before F^- adsorption to 3,495 cm^{-1} after F^- adsorption, indicating the hydroxyl group involved in the fluorine adsorption processes. The extra peaks appeared at 489 cm^{-1} indicated the presence of –AlF, which showed fluoride was adsorbed on the surface of AC-Z [45].

Fig. 11 describes the fluoride adsorption mechanism through a schematic diagram. EDS and FTIR Characterization tests were conducted to investigate the element

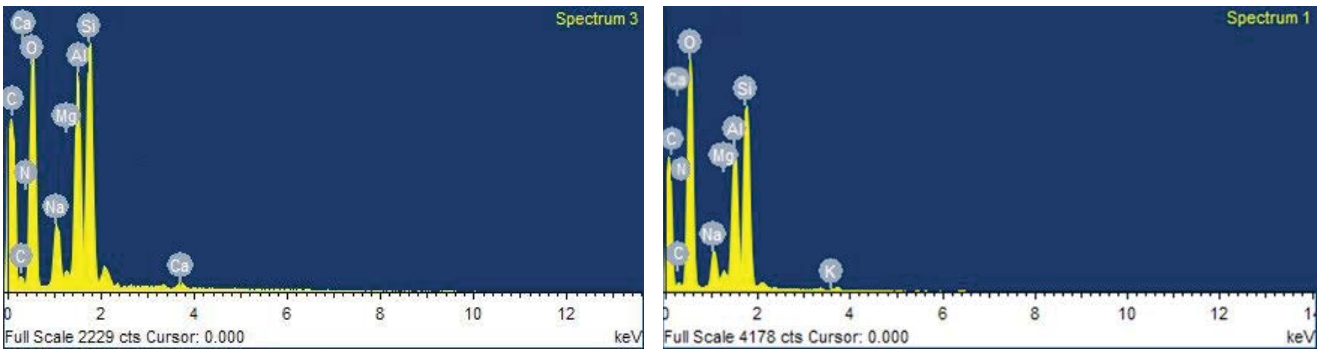

Fig. 9. EDS energy spectrum (a) before and (b) after AC-Z adsorption.

Table 6
Analysis of specific surface area

Sample	BET surface area (m^2/g)	Pore volume (cm^3/g)	Average pore diameter (nm)
Zeolite molecular sieve	13.3953	0.0409	25.8975
AC-Z	47.0075	0.1198	11.1767

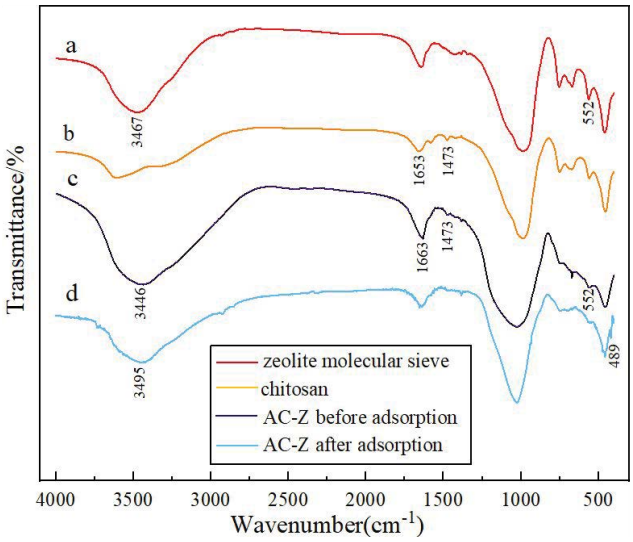

Fig. 10. FTIR spectra of zeolite molecular sieve (a), chitosan (b), AC-Z before (c) and after adsorption (d).

and functional groups presented on the surface of AC-Z adsorbents before and after fluoride adsorption. From EDS analysis, it was confirmed the element of aluminium had a predominant contribution in enhancing the fluoride adsorption efficiency [46]. Due to aluminum modified zeolite molecular sieve, the inner surface of AC-Z adsorbents had large specific surface area (BET surface area of 47.0075 m^2/g), and it was easy for fluoride ions to enter the inside of the adsorbent through diffusion [47]. From FTIR analysis, aluminium was presented mostly in form of Al–OH on AC-Z adsorbents, which caused increasing uptake capacity of adsorbents [48]. One aluminum has six coordination bonds, Al–OH in zeolite molecular sieves can be protonated and had ion exchange reaction with six fluoride ions [49]. On the other hand, aluminum formed coordination bonds with amino groups and hydroxyl groups on the surface of chitosan during the preparation process. During the reaction with fluoride ions, F^- replaced hydroxyl groups and formed Al–F bonds with aluminum, which increased the adsorption ability of AC-Z composites [50].

3.12. Regeneration

Fig. 12a shows the effect of different regenerants on AC-Z fluoride removal efficiency and adsorption capacity after regeneration. The order of fluoride removal performance by regenerants was NaOH > $AlCl_3$ > NaCl > HCl > Na_2SO_4. The fluoride removal rate and adsorption capacity were 81.5% and 0.35 mg/g respectively, with 1 mol/L NaOH as the regenerant which was the best among five regenerants. AC-Z was used for fluoride removal and regenerated for 6 times to investigate the long-term adsorption performance. As shown in Fig. 12b, AC-Z regenerated by NaOH solution showed higher fluoride removal rate after 6 times repeated regeneration.

3.13. Application of AC-Z adsorbents

Natural groundwater containing 9.2 mg/L fluoride was collected from a well found in Kangping city, Liaoning, China. The physical and chemical characteristics of the samples were shown in Table 7. Batch adsorption experiment was carried out for the well sample waters without adjusting the pH (pH 6.80). The experiment was accomplished at optimal conditions of dose 2.0 mg/100 mL and

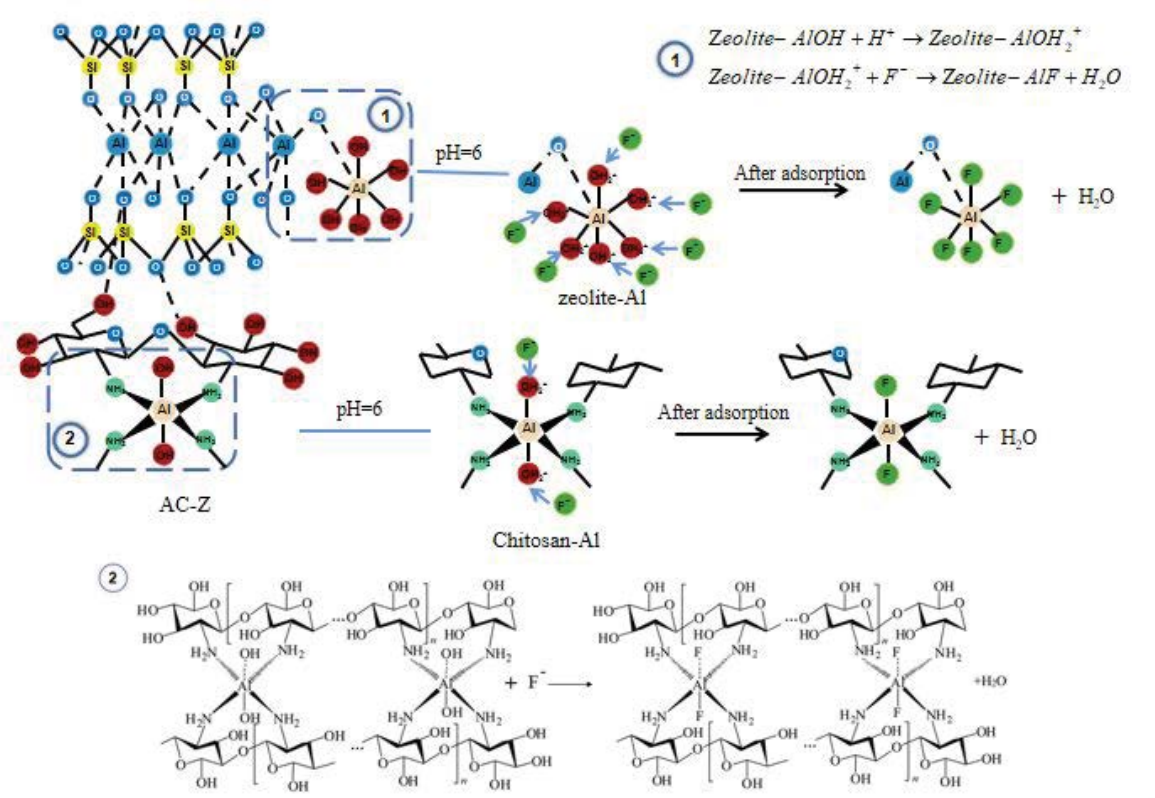

Fig. 11. The proposed fluoride adsorption mechanism of AC-Z.

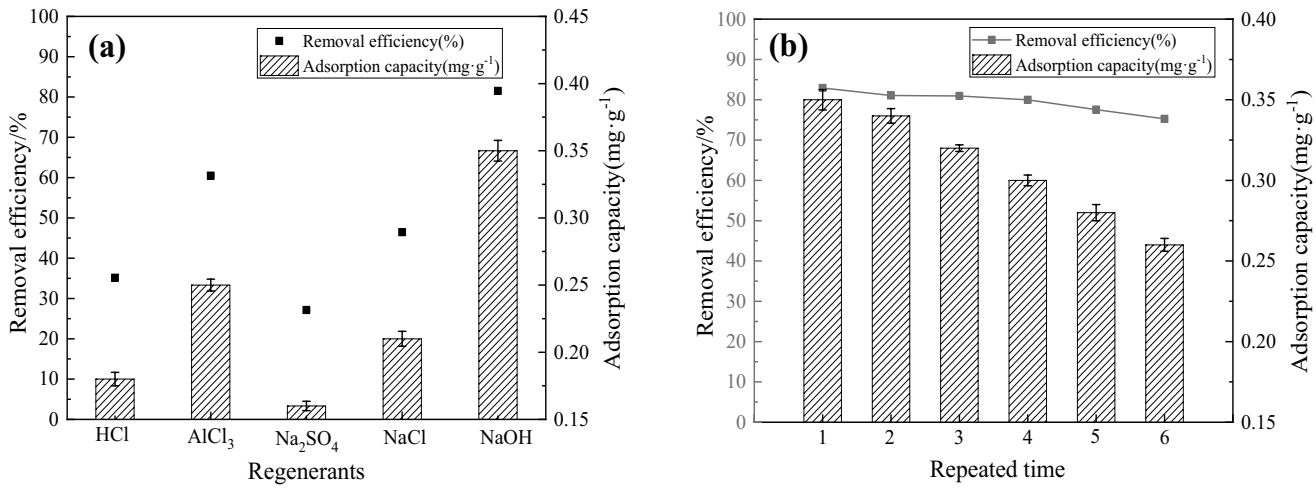

Fig. 12. Effects of regenerants (a) and repeated times (b) on AC-Z performance of fluoride removal.

contact time 8 h. Co-existing anions and cations were also checked before and after AC-Z adsorption. The results showed AC-Z was effective for fluoride adsorption with concentration reducing from 9.2 to 0.84 mg/L which below the standard level. The co-existing ions had little influence on fluoride removal, and concentration of Cl^-, SO_4^{2-}, Fe^{2+}, Mn^{2+} in treated water all met the standard requirements. It was also investigated that the residual aluminum ion leached from AC-Z at optimum conditions was found to be 0.02 mg/L, which was by far less than the China Drinking Water Standard (0.2 mg/L).

4. Conclusion

A low-cost and environmental-friendly adsorbent was prepared by loading aluminium onto the chitosan modified zeolite molecular sieve particles (AC-Z). The prepared AC-Z adsorbents reached a high removal efficiency

Table 7
Physical and chemical characteristics of groundwater in Liaoning province, China

Samples	pH	F	Cl^-	SO_4^{2-}	Fe^{2+}	Mn^{2+}	Al^{3+}
				mg/L			
Groundwater	6.80	9.2	61.3	45.7	1.47	0.95	–
Treated water	7.10	0.84	5.6	8.9	0.13	0.05	0.02
Standard	6.5–8.5	<1.0	<250	<250	<0.3	<0.1	<0.2

of 92% with initial fluoride concentration of 10 mg/L, dose of 2 g/100 mL, contact time of 8 h, pH value of 7 and temperature of 20°C. And the residual aluminum concentration after defluoridation by AC-Z was found to be 0.02 mg/L which is by far lower than China Drinking Water Standard (0.2 mg/L). Based the results of characterization of EDS and FITR, aluminium on AC-Z particles have significant contribution in fluoride removal. The adsorption mechanism was due to the co-operative action of Al-OH function group and hydroxyl for fluoride ion-exchange. The regeneration study illustrated that AC-Z adsorbents had good adsorption capacity after regenerated by NaOH (1 mol/L) solution. Future research on this AC-Z adsorbent will focus on optimizing dynamic processes to provide technical parameters for large-scale production applications.

Acknowledgement

The authors are thankful to National Natural Science Foundation of China (51508342).

References

[1] W. Wang, N.F. Mwiathi, C. Li, W. Luo, X. Zhang, Y. An, M. Zhang, P. Gong, J. Liu, X. Gao, Assessment of shallow aquifer vulnerability to fluoride contamination using modified AHP-DRASTICH model as a tool for effective groundwater management, a case study in Yuncheng Basin, China, Chemosphere,286(2022)131601,doi:10.1016/j.chemosphere.2021.131601.
[2] T. Wang, D. Sun, Q. Zhang, Z. Zhang, China's drinking water sanitation from 2007 to 2018: a systematic review, Sci. Total Environ., 757 (2020) 143923, doi: 10.1016/j.scitotenv.2020.143923.
[3] J. Li, H. Zhou, K. Qian, X. Xie, X. Xue, Y. Yang, Y. Wang, Fluoride and iodine enrichment in groundwater of North China Plain: evidences from speciation analysis and geochemical modeling, Sci. Total Environ., 598 (2017) 239–248.
[4] WHO, Guidelines for Drinking-Water Quality, 4th ed., World Health Organization, 2011.
[5] National Health Commission of the People's Republic of China, Standard of Drinking Water Quality, Beijing, 2016 (in Chinese).
[6] V. Kimambo, P. Bhattacharya, F. Mtalo, J. Mtamba, A. Ahmad, Fluoride occurrence in groundwater systems at global scale and status of defluoridation – state of the art, Groundwater Sustainable Dev., 9 (2019) 100223, doi: 10.1016/j.gsd.2019.100223.
[7] A.A. Alcaine, C. Schulz, J. Bundschuh, G. Jacks, R. Thunvik, J.-P. Gustafsson, C.-M. Mörth, O. Sracek, A. Ahmad, P. Bhattacharya, Hydrogeochemical controls on the mobility of arsenic, fluoride and other geogenic co-contaminants in the shallow aquifers of northeastern La Pampa Province in Argentina, Sci. Total Environ., 715 (2020) 136671, doi: 10.1016/j.scitotenv.2020.136671.
[8] S. Alkurdi, R.A. Al-Juboori, J. Bundschuh, I. Hamawand, Bone char as a green sorbent for removing health threatening fluoride from drinking water, Environ. Int., 127 (2019) 704–719.
[9] J. He, Y. Yang, Z. Wu, C. Xie, K. Zhang, L. Kong, J. Liu, Review of fluoride removal from water environment by adsorption, J. Environ. Chem. Eng., 8 (2020) 104516, doi: 10.1016/j.jece.2020.104516.
[10] P. Pillai, S. Dharaskar, S. Pandian, H. Panchal, Overview of fluoride removal from water using separation techniques, Environ. Technol. Innovation, 21 (2021) 101246, doi: 10.1016/j.eti.2020.101246.
[11] A. Dhillon, S. Prasad, D. Kumar, Recent advances and spectroscopic perspectives in fluoride removal, Appl. Spectrosc. Rev., 52 (2017) 175–230.
[12] S.I. Bouhadjar, H. Kopp, P. Britsch, S.A. Deowan, J. Hoinkis, J. Bundschuh, Solar powered nanofiltration for drinking water production from fluoride-containing groundwater – a pilot study towards developing a sustainable and low-cost treatment plant, J. Environ. Manage., 231 (2019) 1263–1269.
[13] O.Z. Ojekunle, O.V. Ojekunle, A.A. Adeyemi, A.G. Taiwo, O.R. Sangowusi, A.M. Taiwo, A.A. Adekitan, Evaluation of surface water quality indices and ecological risk assessment for heavy metals in scrap yard neighbourhood, SpringerPlus., 5 (2016) 560, doi: 10.5004/dwt.2022.28082.
[14] F.D. Belkada, O. Kitous, N. Drouiche, S. Aoudj, O. Bouchelaghem, N. Abdi, H. Grib, N. Mameri, Electrodialysis for fluoride and nitrate removal from synthesized photovoltaic industry wastewater, Sep. Purif. Technol., 204 (2018) 108–115.
[15] Y. Gao, M. Li, Y. Ru, J. Fu, Fluoride removal from water by using micron zirconia/zeolite molecular sieve: characterization and mechanism, Groundwater Sustainable Dev., 13 (2021) 100567, doi: 10.1016/j.gsd.2021.100567.
[16] C.F.Z. Lacson, M. Lu, Y. Huang, Fluoride-containing water: a global perspective and a pursuit to sustainable water defluoridation management – an overview, J. Cleaner Prod., 280 (2020) 124236.
[17] Y. Gao, J. Zhang, Chitosan modified zeolite molecular sieve particles as a filter for ammonium nitrogen removal from water, Int. J. Mol. Sci., 21 (2020) 2382, doi: 10.3390/ijms21072383.
[18] A. Goswami, M.K. Purkait, Kinetic and equilibrium study for the fluoride adsorption using pyrophyllite, Sep. Sci. Technol., 46 (2011) 1797–1807.
[19] S.S. Tripathy, A.M. Raichur, Abatement of fluoride from water using manganese dioxide-coated activated alumina, J. Hazard. Mater., 153 (2008) 1043–1051.
[20] T. Rafique, K.M. Chadhar, T.H. Usmani, S.Q. Mermon, K. Shirin, S. Kamaluddin, F. Soomro, Adsorption behavior of fluoride ion on trimetal-oxide adsorbent, Desal. Water Treat., 56 (2015) 1669–1680.
[21] N.N.A. Malek, A.H. Jawad, K. Ismail, R. Razuan, Z.A. ALOthman, Fly ash modified magnetic chitosan-polyvinyl alcohol blend for reactive orange 16 dye removal: adsorption parametric optimization, Int. J. Biol. Macromol., 189 (2021) 464–476.
[22] S. Afshin, Y. Rashtbari, M. Shirmardi, M. Vosoughi, A. Hamzehzadeh, Adsorption of basic violet 16 dye from aqueous solution onto mucilaginous seeds of *Salvia sclarea*: kinetics and isotherms studies, Desal. Water Treat., 161 (2019) 365–375.
[23] J.C. Burillo, L. Ballinas, G. Burillo, E.G. Lestarjette, D.L. Gutierrez, H.S. Hidalgo, Chitosan hydrogel synthesis to remove arsenic and fluoride ions from groundwater, J. Hazard. Mater, 417 (2021)126070, doi: 10.1016/j.jhazmat.2021.126070.

[24] S. Jagtap, M. Yenkie, N. Labhsetwar, S. Rayalu, Defluoridation of drinking water using chitosan based mesoporous alumina, Microporous Mesoporous Mater., 142 (2011) 454–463.
[25] Y.D. Wirtu, F. Melak, M. Yitbarek, H. Astatkie, Aluminum coated natural zeolite for water defluoridation: a mechanistic insight, Groundwater Sustainable Dev., 12 (2021) 100525, doi: 10.1016/j.gsd.2020.100525.
[26] A. Teimouri, S.G. Nasab, N. Vahdatpoor, S. Habibollahi, H. Salavati, A.N. Chermahini, Chitosan/zeolite Y/Nano ZrO_2 nanocomposite as an adsorbent for the removal of nitrate from the aqueous solution, Int. J. Biol. Macromol., 93 (2016) 254–266.
[27] R.N. Tabi, F.O. Agyemang, K. Mensah-Darkwa, E.K. Authur, E. Gikunoo, F. Momade, Zeolite synthesis and its application in water defluorination, Mater. Chem. Phys., 261 (2021) 124229, doi: 10.1016/j.gsd.2020.100525.
[28] W.M.A. Rouby, A.A. Farghali, M.A. Sadek, W.F. Khalil, Fast removal of Sr(II) from water by graphene oxide and chitosan modified graphene oxide, J. Inorg. Organomet. Polym. Mater., 28 (2018) 1–14.
[29] G. Asgari, B. Roshani, G. Ghanizadeh, The investigation of kinetic and isotherm of fluoride adsorption onto functionalize pumice stone, J. Hazard. Mater., 217–218 (2012) 123–132.
[30] F. Zewge, Combined aluminium sulfate/hydroxide process for fluoride removal from drinking water, Bull. Chem. Soc. Ethiop., 30 (2017) 391–401.
[31] K. Zhang, S. Wu, X. Wang, J. He, B. Sun, Y. Jia, T. Luo, F. Meng, Z. Jin, D. Lin, W. Shen, L. Kong, J. Liu, Wide pH range for fluoride removal from water by MHS-MgO/$MgCO_3$ adsorbent: kinetic, thermodynamic and mechanism studies, J. Colloid Interface Sci., 446 (2015) 194–202.
[32] M. Chaudhary, P. Bhattacharya, A. Maiti, Synthesis of iron oxyhydroxide nanoparticles and its application for fluoride removal from water, J. Environ. Chem. Eng., 4 (2016) 4897–4903.
[33] B.H. Hameed, D.K. Mahmoud, A.L. Ahmad, Equilibrium modeling and kinetic studies on the adsorption of basic dye by a low-cost adsorbent: coconut (*Cocos nucifera*) bunch waste, J. Hazard. Mater., 158 (2008) 65–72.
[34] A.M. Raichur, M.J. Basu, Adsorption of fluoride onto mixed rare earth oxides, Sep. Purif. Technol., 24 (2001) 121–127.
[35] S. Raghav, D. Kumar, Comparative kinetics and thermodynamic studies of fluoride adsorption by two novel synthesized biopolymer composites, Carbohydr. Polym., 203 (2019) 430–440.
[36] S. Raghav, S. Nehra, D. Kumar, Adsorption removal studies of fluoride in aqueous system by bimetallic oxide incorporated in cellulose, Process Saf. Environ. Prot., 127 (2019) 211–225.
[37] Y. Nie, C. Hu, C. Kong, Enhanced fluoride adsorption using Al(III) modified calcium hydroxyapatite, J. Hazard. Mater., 233–234 (2012) 194–199.
[38] E. Kusrini, N. Sofyan, N. Suwartha, G. Yesya, C.R. Priadi, Chitosan-praseodymium complex for adsorption of fluoride ions from water, J. Rare Earths, 33 (2015) 1104–1113.
[39] Y. Lai, K. Yang, C. Yang, Z. Tian, W. Guo, J. Li, Thermodynamics and kinetics of fluoride removal from simulated zinc sulfate solution by La(III)-modified zeolite, Trans. Nonferrous Met. Soc. China, 28 (2018) 783–793.
[40] R. Han, J. Zhang, H. Pan, Y. Wang, Z. Zhao, M. Tang, Study of equilibrium, kinetic and thermodynamic parameters about methylene blue adsorption onto natural zeolite, Chem. Eng. J., 145 (2009) 496–504.
[41] M. Kara, H. Yuzer, E. Sabah, M.S. Celik, Adsorption of cobalt from aqueous solutions onto sepiolite, Water Res., 37 (2003) 224–232.
[42] S. Somderam, A.S. Abd Aziz, A.H. Abdullah, R. Mat, Characterisation of NaA zeolite made from Malaysian kaolin, Chem. Eng. Trans., 72 (2019) 325–330.
[43] A.H. Jawad, A.S. Abdulhameed, N.N.A. Malek, Z.A. ALOthman, Statistical optimization and modeling for color removal and COD reduction of reactive blue 19 dye by mesoporous chitosan-epichlorohydrin/kaolin clay composite, Int. J. Biol. Macromol., 164 (2020) 4218–4230.
[44] A.H. Jawad, A.S. Abdulhameed, R. Abdallah, Z.M. Yaseen, Zwitterion composite chitosan-epichlorohydrin/zeolite for adsorption of methylene blue and reactive red 120 dyes, Int. J. Biol. Macromol., 163 (2020) 756–765.
[45] S. Kanrar, S. Debnath, P. De, K. Parashar, K. Pillay, P. Sasikumar, U.C. Ghosh, Preparation, characterization and evaluation of fluoride adsorption efficiency from water of iron-aluminium oxide-graphene oxide composite material, Chem. Eng. J., 306 (2016) 269–279.
[46] M. Dessalegne, F. Zewge, I. Diaz, Aluminum hydroxide supported on zeolites for fluoride removal from drinking water, J. Chem. Technol. Biotechnol., 92 (2016) 605–613.
[47] S. Mukherjee, S. Barman, G. Halder, Fluoride uptake by zeolite NaA synthesized from rice husk: isotherm, kinetics, thermodynamics and cost estimation, Groundwater Sustainable Dev., 7 (2018) 39–47.
[48] Y. Gao, Y. Ru, L. Zhou, X. Wang, J. Wang, Preparation and characterization of chitosan-zeolite molecular sieve composite for ammonia and nitrate removal, Adv. Compos. Lett., 27 (2018) 185–192.
[49] D. Si, M. Zhu, X. Sun, M. Xue, Y. Li, T. Wu, T. Gui, I. Kumakiri, X. Chen, H. Kita, Formation process and pervaporation of high aluminum ZSM-5 zeolite membrane with fluoride-containing and organic template-free gel, Sep. Purif. Technol., 257 (2021) 117963, doi: 10.1016/j.seppur.2020.117963.
[50] C. Shen, C. Hui, S. Wu, Y. Wen, L. Li, Z. Jiang, M. Li, W. Liu, Highly efficient detoxification of Cr(VI) by chitosan-Fe(III) complex: process and mechanism studies, J. Hazard. Mater., 244–245 (2013) 689–697.